# The 2006 Kythira (Greece), $M_w$6.7 slab-pull event: tectonic implications and the geometry of the hellenic wadati-benioff zone

**Irini Nikolintaga** ([1]), **Vassilis Karakostas** ([1]), **Eleftheria Papadimitriou** ([1]) **and Filippos Vallianatos** ([2])
([1]) *Geophysics Department, School of Geology, Aristotle University of Thessaloniki, Greece*
([2]) *Technological Educational Institute of Crete, Department of Natural Resources & Environment, Geophysics & Seismology Laboratory, Crete, Greece*

**Abstract**
A strong ($M_w$=6.7) intermediate depth earthquake occurred on 8 January 2006 (11:34 UTC) in southwestern Aegean Sea (Greece) causing limited damage to structures on the nearby islands of Kythira and Antikythira, as well as western Crete Island. The epicentral area belongs to the SW segment of the Hellenic Arc, which is known to be associated with the occurrence of large shallow and intermediate depth earthquakes, mainly due to the subduction of the Eastern Mediterranean oceanic lithosphere under the Aegean microplate. The main shock occurred on a dextral strike slip fault at a depth of 75 km, within the descending slab, as it is revealed by both, the spatial distribution of the accurately located aftershocks and its fault plane solution determined in the present study and implying a slab-pull event. The aftershock activity from 8 to 31 January 2006 is distributed in depths ranging from 55 to 75 km, and being comprised in an almost rectangular and vertical plane with a length equal to 28 km and a width of 20 km, which adequately defines the dimensions of the rupture area. The geometry of the Wadati-Benioff zone in this area, namely the southwestern part of the Hellenic Arc, is explored by an exhaustive analysis of all the available phase arrivals gathered from the International Seismological Centre, and the relocation of the earthquakes occurred since 1964 in the South-West Aegean region.

**Key words** *Hellenic Arc – subduction zone geometry – slab-pull event*

## 1. Introduction

On 8 January 2006, a strong intermediate depth earthquake ($M_w$=6.7) occurred in the southwestern part of the Hellenic Arc (fig. 1). The main shock epicenter is located at 36.208°N–23.445°E near the Island of Kythira, at a depth of 75 km (hypocenter determined in the present study). The broader epicentral area had been identified as the probable source of a future strong earthquake by Papazachos *et al*. (2002) and Tzanis and Vallianatos (2003), who independently investigated and detected accelerated moment release. The relatively large main shock magnitude resulted to be strongly felt in southern Greece, as well as in southern Italy, Egypt, Cyprus, Turkey, Israel, Lebanon, Syria, and Jordan. Nevertheless, there were no casualties, but only some limited damages to infrastructure in the area of Kythira and the city of Chania (NW Crete) were reported. The peak ground acceleration (PGA) recorded on the island of Kythira was rather small ($a_g$=0.12g) (ITSAK, 2006), due to the intermediate depth origin of the main shock.

*Mailing address*: Dr. Vassilis Karakostas, Geophysics Department, School of Geology, Aristotle University of Thessaloniki, GR54124 Thessaloniki, Greece; e-mail: vkarak@geo.auth.gr

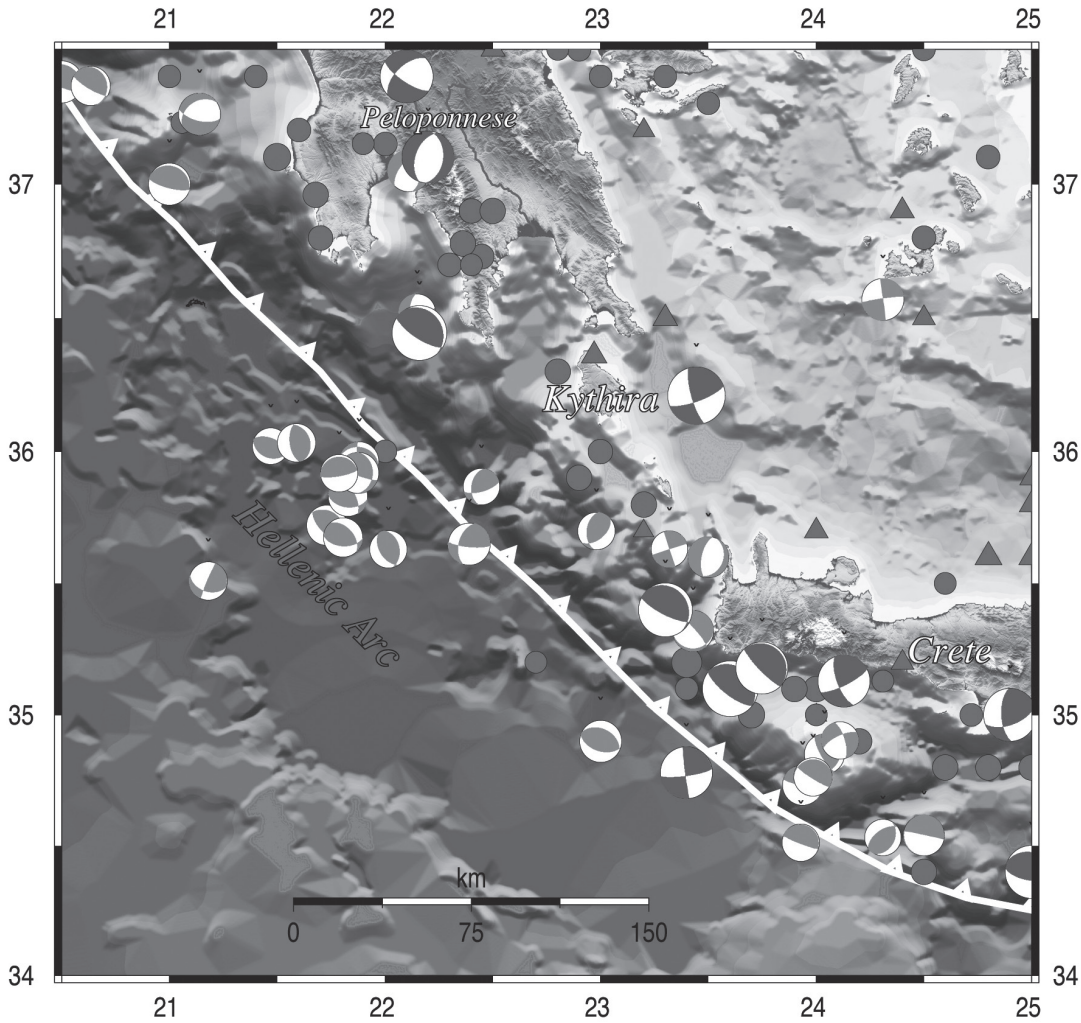


**Fig. 1.** The main seismotectonic and structural features of the SW Hellenic Arc and Trench system. The epicenters of the historical known earthquakes both shallow (circles) and intermediate ones (triangles) with M>6.0 are also shown along with the available fault plane solutions as lower hemisphere equal area projection for events of M>6.0 (in dark grey) and of smaller magnitude ones (in light grey).

South Aegean is one of the most active plate margins of the Mediterranean area, exhibiting high seismicity and having a long historical record of devastating shallow interplate earthquakes with magnitudes up to about 8.3 (Papazachos and Papazachou, 2003). Prominent geotectonic feature of the broader area is the Hellenic Trench, where the Eastern Mediterranean oceanic lithosphere (front part of the African plate) is subducted under the Aegean microplate, forming an inclined zone of seismicity, dipping to the inner, concave, part of the trench, to a depth of about 150-200 km (Papazachos and Comninakis, 1970, 1971; Papazachos, 1990; Papazachos *et al*., 2000). To the north-east of the Trench, the Hellenic Arc

(Peloponnese-Kythira-Crete) comprises the accretionary prism and farther north, the Southern Aegean basin (Cretan Sea) and the Volcanic Arc (fig. 1).

The intermediate-depth seismicity along the southwestern part of the Hellenic Arc outlines the subducting slab, whereas shallower thrust-faulting seismicity depicts an active seismogenic subduction interface. This part of the Hellenic Arc is associated with moderate arc-parallel extension and strong compression perpendicular to the subduction front (Kahle *et al*., 1998). The convergence rate, approximately equal to 4.5 cm/yr, is fast enough to produce a degree of roll-back at the Hellenic Trench (Le Pichon and Angelier, 1979), leading to stretching of the overriding plate. The strain tensor based on the moment tensor sum for the Aegean back-arc shows that overall this region is stretching in approximately a north-south direction and thinning both vertically and in the east-west direction (Sonder and England, 1986). The back-arc stretching direction is therefore oblique to the trench roll-back direction.

All the reliable known focal mechanisms of the strong earthquakes that occurred in the western and southern part of the Hellenic arc are shown in fig. 1, as an equal area lower hemisphere projection. Reverse and low angle thrust faulting dominates along the Hellenic Trench, with the P axis having a constant direction almost perpendicular to the strike of the Hellenic Arc, as it already is mentioned above, in along its western and central parts. Shallow earthquakes (depths up to 60 km) occur on faults striking in a NW-SE direction, and dipping from the convex to the concave side of the arc. Normal faulting characterizes the inner part of the arc with N-S striking faults and E-W trending T-axes, resulting to along-arc extension at depths up to 40 km (Papazachos *et al*., 1998; Benetatos *et al*., 2004). The intermediate depth earthquakes are associated with strike–slip faulting with a considerable thrust component. The P axes are parallel to the strike of the Hellenic Arc, while the T axes are normal to this strike and parallel to the dip direction of the Benioff zone (Kiratzi and Papazachos, 1995; Benetatos *et al*., 2004). Bohnhoff *et al*. (2005) claim that the fault plane solutions for earthquakes within the dipping lithosphere indicate the slab pull as the dominant force within the subduction process, responsible for the roll–back of the Hellenic subduction zone.

Previous studies (*e.g*. Hatzfeld and Martin, 1992; Knapmeyer, 1999; Papazachos *et al*., 2000) using earthquake hypocenters have revealed a well-developed Wadati-Benioff zone dipping inward towards the central Aegean Sea up to depths of about 150 to 200 km. The slab is descending at an angle of about 30° up to the depth of 100 km, while it becomes steeper (~45°) in greater depths. Seismic tomography studies provide a deeper image of the subducted slab, which can be followed further to the north–east down to 600 km (Papazachos *et al*., 1995; Alessandrini *et al*., 1997; Wortel and Spakman, 2000).

The 2006 seismic excitation motivated the detailed study of the activated area, aiming to highlight the geometry of the descending slab. The aftershocks were relocated by the use of high quality seismological data and a new 1D velocity model of the P-waves at the southwestern part of the Hellenic Arc. Based on the accurate hypocentral locations of the 2006 Kythira main shock and its aftershock sequence, we anticipate a detailed description of the main rupture properties and contribution to the configuration of the subducted slab in this side of the Hellenic Arc. By extending our efforts to a broader area of the Hellenic Wadati-Benioff Zone, all the available phases of P- and S-waves published by the International Seismological Center are used for the relocation of the earthquakes occurred inside the rectangle between 34°-38°N and 20°-25.5°E, during January 1964-March 2007.

## 2. Seismological Data Used

Two different data sets were used in this work in order to study the aftershock sequence of the Kythira earthquake and to improve the hypocentral accuracy in the southwestern part of the Hellenic Arc. The first data set consists of the recordings at stations of local and regional seismological networks (fig. 2a), of the aftershock sequence for the period 8-31 January

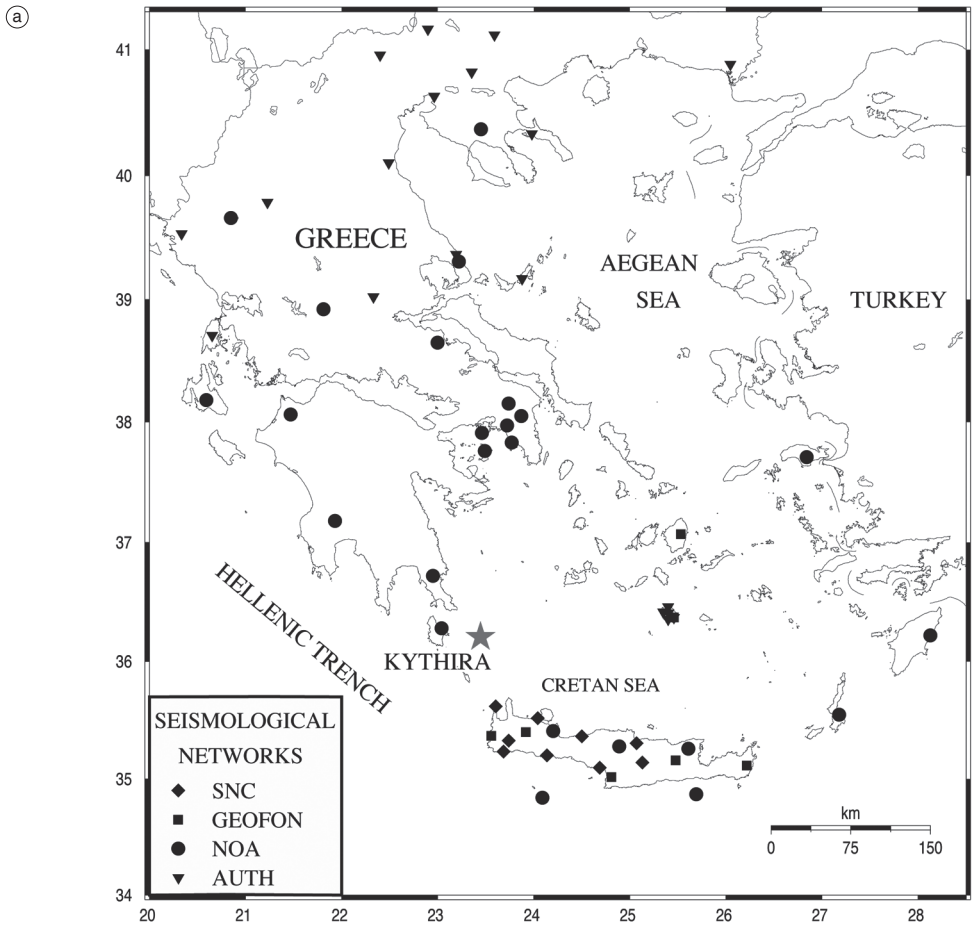


**Fig. 2a,b.** a) Sites of the seismological stations used: diamonds represent the station sites of the SNC network, whereas squares represent the sites of the GEOFON seismological stations, circles the stations of the National Observatory of Athens, and reverse triangles the stations of the Seismological Network of Geophysics Department, AUTH. b) Sites of the regional stations in Greece and the neighboring countries. Triangles and squares depict the seismological stations installed before and after 1981, respectively.

2006, when the seismic activity rate was the highest. The second data set comprises the recordings at regional stations in Greece and the neighboring countries (fig. 2b) of all the available arrival times of the earthquakes contained in the International Seismological Centre archives.

More particularly, the main volume of data for the focal parameters determination of the 2006 Kythira main shock and its aftershock activity is provided by the short period three-component stations of the digital Seismological Network of Crete (SNC), operated by the Laboratory of Geophysics and Seismology (LGS) of the Technological and Educational Institute of Crete since the end of 2003. It consists of 10 operational stations (nine short period and one broad-band station) equipped by high resolution 24-bits digitizers, Reftek 130 type and three-component Guralp CMG-40T and Sercel L-4-3D, 1Hz, sensors. This local network provided a wealth of data for the aftershock activ-

**Fig. 2a,b.** (*continued*)

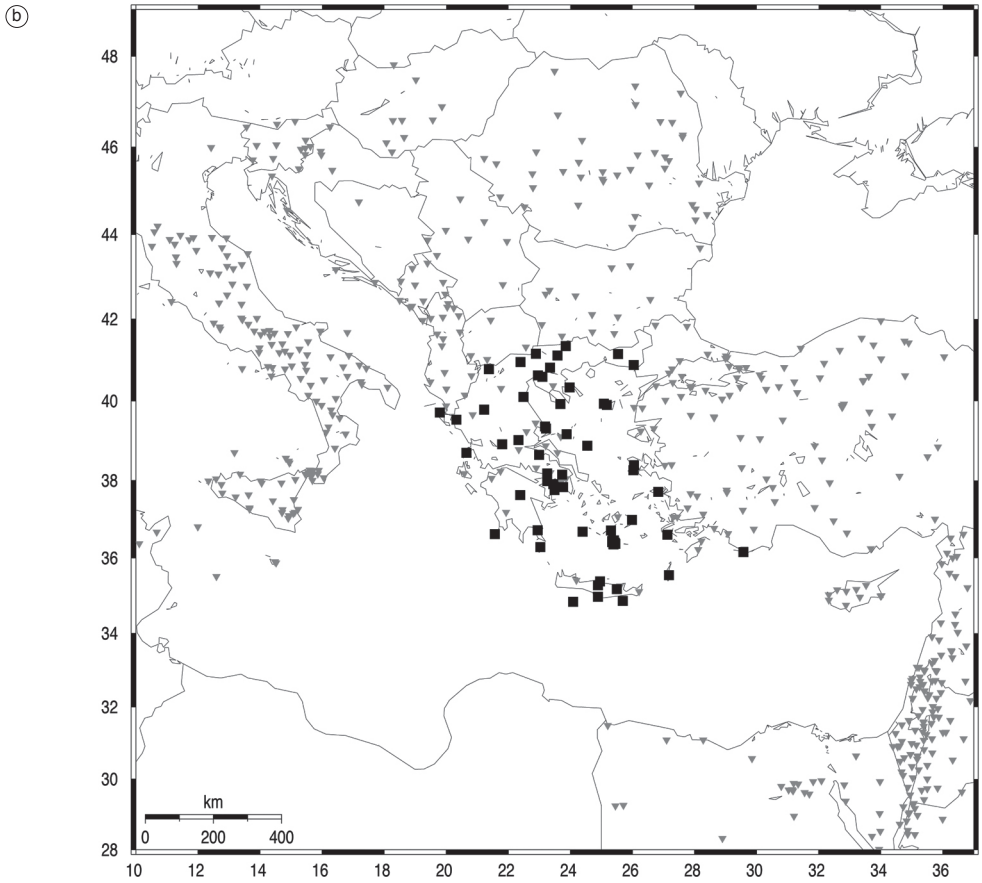


ity, which lasted approximately three weeks. In addition to these data all the available waveforms from the seismological stations located in south Aegean and maintained by the GEOFON network were collected and manually analyzed. Moreover, the arrival times of the earthquakes also recorded at the permanent seismological stations of the Geodynamic Institute of National Observatory of Athens and the waveforms recorded at the stations of the Seismological Network of Geophysics Department, Aristotle University of Thessaloniki were used (fig. 2a).

The proximity of the local seismological stations to the epicentral area and the adequate azimuthal coverage of the study area for most of the aftershocks that were strong enough to be recorded by the regional network, ensured the accurate determination of the focal parameters and especially of the focal depths not only of the main shock itself, but also for the majority of its aftershocks. The histograms of fig. 3 show the epicentral distances of the closest station for all the recorded aftershocks (fig. 3a) and the maximum angle (GAP) between the epicenter and two successive stations (fig. 3b). In most of the cases, the closest station to the epicenter is located at a distance of less than 50 km, whereas almost all stations that detected an earthquake leave an azimuthal gap of less than 180º.

For the relocation of the relatively high seismic activity taking place in the broader study area, the online bulletin of International Seismo-

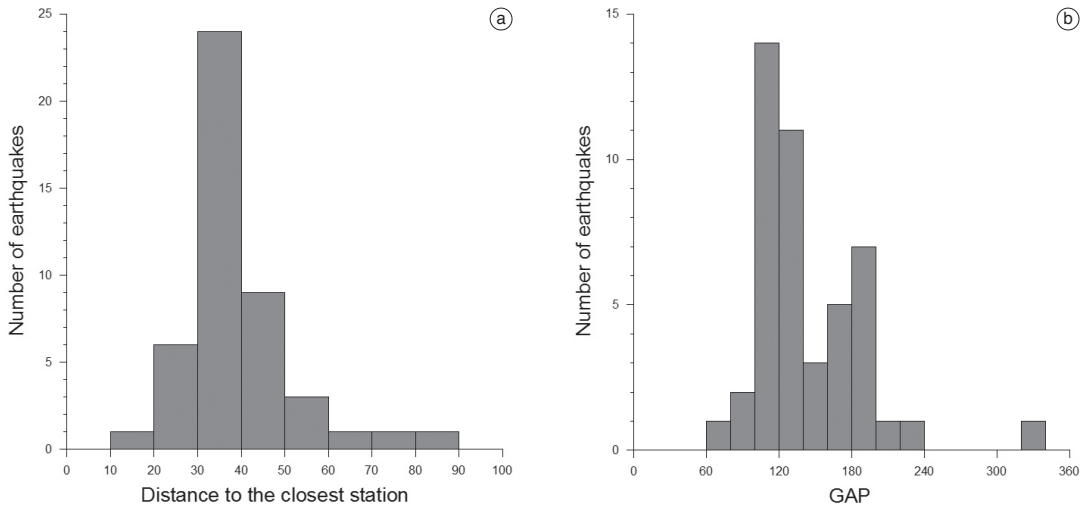


**Fig. 3a,b.** a) Histogram of the epicentral distances of the closest station for all the recorded aftershocks and b) of the maximum angle (GAP) between the epicenter and two successive stations.

logical Center (http://www.isc.ac.uk/), including phases since 1964, was used to retrieve the recordings of the regional events in the last decades. All the arrival times of the P– and S–waves recorded at seismological stations in epicentral distances up to 10° were collected, creating in that way a large data set of 14.457 earthquakes, with magnitudes ranging from 2.4 to 6.5. Due to the small number of seismological stations in Greece during the first years of our study, the quality of our data sample is rather poor. However, the gradual installation of new seismological stations resulted to the improvement of data quality, especially after 1981. On the map of fig. 2b, grey triangles are used to depict the seismological stations installed before 1981, while black squares for the stations in Greece installed since 1981 and afterwards.

## 3. Event Relocation Procedure

Earthquakes from both the aftershock sequence and the regional seismicity were located with the HYPOINVERSE computer program (Klein, 2002). However, because the epicentral distances of the available seismological stations differ considerably in each case, two different velocity models were used. For the aftershock sequence, a velocity model consisting of five layers above a half space (table I) is adopted. This model was introduced by Nikolintaga *et al*. (2007) up to the depth of 50 km and is based on the travel time curves of many earthquakes, which occurred in the adjacent area and were recorded at several stations of the SNC and GEOFON networks. For the relocation of the regional seismicity, the regional velocity model proposed by Panagiotopoulos and Papazachos (1985) was used, being composed of two layers above a half space ($v_g$=6 km*s$^{-1}$, $d_g$=19 km, $v_b$=6.6 km*s$^{-1}$, $d_b$=12 km, $v_n$=7.9 km*s$^{-1}$, $d_n$=∞). Since the two aforementioned models initially provided information on the shallower layers only, information concerning the velocity structure of the upper mantle was taken from Papazachos *et al*. (2000) who suggested a model based on tomographic results of Papazachos and Nolet (1997). For obtaining the shear wave velocities, the mean velocity ratio is assumed to be equal to $\mathbf{v_p}/v_s$=1.78±0.01, as it is determined by Nikolintaga *et al*. (2007) by individual Wadati plots. This value is in agreement with the results from previous studies conducted in the same area (*e.g*. 1.79 obtained by Hatzfeld *et al*., 1990; 1.80 by de Chabalier *et al*., 1992).

**Table I.** Velocity model used for the earthquake location in the south-western Aegean area (Nikolintaga *et al*., 2007).

| VP (km/s) | VP (km/s) |
|---|---|
| 5.9 | 0.00 |
| 6.54 | 11.00 |
| 7.92 | 30.00 |
| 7.95 | 50.00 |
| 8.00 | 100.00 |
| 8.05 | 120.00 |

Using a one-dimension velocity model two major problems are raised. The first one is due to the lateral heterogeneities of the real structure. Calculating time residuals and using them as corrections in each seismological station, it is possible to take into account the deviations between the real structure and the theoretical model. The second problem is due to the dimensions of the area under study. If this is a small one, then the ray paths from each earthquake to a certain station are almost the same, thus permitting the calculation of a reliable mean value of the time residual. If the area under study is relatively large, then the epicentral distances and the ray paths of different earthquakes to the same station differ considerably and the calculated time residuals cannot contribute to the location accuracy. The use of the HYPOINVERSE program provides the feasibility of overcoming this problem, because the area under study can be divided into smaller parts. For each sub area different velocity model and time residuals can be used.

In the present study, station corrections were calculated for the aftershock sequence without any sub division in smaller areas since the aftershock area is rather small. The relocation of the regional seismicity was made after separation of the earthquakes in clusters based on their geographical and focal depth distribution. In each case, station corrections are calculated as the mean value of the differences between the observed and the theoretical travel times. This means that time corrections depend on the location and the origin time of the earthquakes before the application of the corrections. To eliminate this problem, the following procedure is followed. Firstly, only the earthquakes with an adequate number of phases and not all of them are used for the calculation of station corrections, since it has been found (*e.g*. Hatzfeld *et al*., 1989) that earthquakes recorded by many stations are located rather independently of the model used. In addition, the initially calculated time residual is used, in an iteratively applied procedure, as time correction and a new value is calculated. This procedure is continued until the time correction is not further changed, and it has reached a stable value. Aiming to examine how the available number of recordings for each event influences the location precision, we tried different data sets. It was observed that in the cases where this number was inadequate the solutions were not stable, meaning that the focal coordinates were continuously changed, thus resulting to increasing time corrections in the repeating iterations.

## 4. Detailed Fault Structure by Relocated Aftershocks

All the available data from 8 to 31 January 2006 were collected and the arrival times for both longitudinal (P) and transverse (S) seismic waves were manually picked for 92 events. Using the accurate hypocentral coordinates of the main shock provided by the recordings of the local network, appropriate station corrections for the reference velocity model were computed. It was preferred to use only the mainshock to calculate station corrections, because its phases are picked with higher accuracy since its magnitude is considerably larger than the magnitudes of the aftershocks.

With the local velocity model of Nikolintaga *et al*. (2007) and the derived station corrections mentioned in the previous paragraph, the hypocentral locations of the aftershocks depicted in fig. 4a, for which 8 or more phases were available, are calculated with the higher possible accuracy (errors in the origin time less than 0.4 s, and errors in both the epicentral (ERH) and focal depth (ERZ) determination less than 10 km). The main shock hypocenter, depicted by star in fig. 4a, is placed at the lower part of the aftershock zone, which is extended in an ENE–WSW

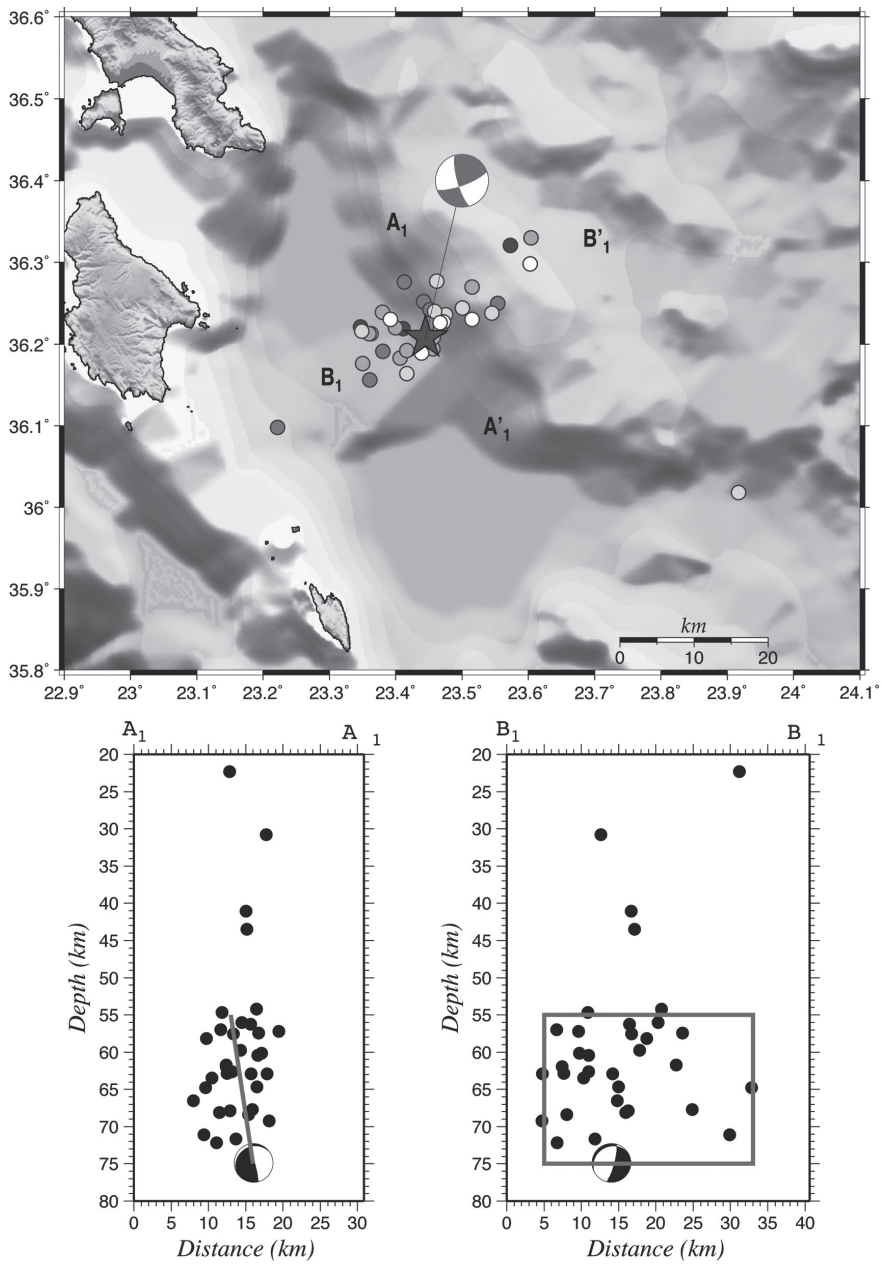


**Fig. 4a,c.** a) Map of the 2006 Kythira main shock (star) and best located aftershocks (circles). The fault plane solution of the main shock is plotted as low-hemisphere equal-area projection and it exhibits strike slip faulting with the fault plane (strike=70°, dip=75° and rake=165°) parallel to the elongated trend of the aftershock zone ($B_1B_2$). b) Cross-section $A_1A_2$, normal to the seismic zone, and c) cross-section $B_1B_2$ parallel to it. Almost all the aftershock hypocenters are located in depths ranging from 55 to 75 km, forming an almost vertical rectangular rupture plane with dimensions of 28 km × 20 km.

direction and has a length of about 28 km, in accordance with fault lengths derived from known scaling laws (*e.g.* Wells and Coppersmith, 1994; Papazachos *et al*., 2004) corresponding to an $M_w$6.7 earthquake. The two cross-sections, one normal to the seismic zone ($A_1A_2$) and the other parallel to it ($B_1B_2$), shown in figs. 4b and 4c, respectively, provide information on the rupture dimensions. Almost all the aftershock hypocenters are located in depths ranging from 55 to 75 km, forming an almost vertical rectangular rupture plane with dimensions of 28 km x 20 km. A few events (4 in total) located in shallower depths (two of them between 40 and 45 km, and the other two at depths of about 30 km and 22 km, respectively), the locations of which remained unalterable even after a detailed check of their arrival times, are not considered to belong to the fault plane of the main shock.

The fault plane solution shown on the map of fig. 4a was determined from the first onsets of the P– waves of all the available local and regional seismological stations, using the FPFIT program (Reasenberg and Oppenheimer, 1985). It exhibits strike slip faulting with one of the planes (with strike=70°, dip=75° and rake=165°) parallel to the elongated trend of the aftershock zone ($B_1B_2$ in fig. 4a) and is considered to be the fault plane. The solution implies that the main shock is along–slab tensional or a slab-pull event. This focal mechanism is also in good agreement with the determinations announced by different Institutes, which in general show dextral strike slip faulting on an ENE–WSW trending fault. It is also in agreement with the representative fault plane solution proposed by Papazachos and Papazachou (2003) on the basis of spatial clustering and focal mechanisms of low magnitude intermediate depth earthquakes. Table II summarizes all the information for the reported focal mechanisms of a typical earthquake of intermediate depth

**Table II.** Representative fault plane solution for intermediate depth earthquakes in the area of Kythira (Papazachos and Papazachou, 2003) and moment tensor solution reported for the Kythira 2006 main shock by different agencies and the solution determined in this study.

| **Nodal plane I** | | | **Nodal plane II** | | | **P – axis** | | **T – axis** | | **Reference** |
|---|---|---|---|---|---|---|---|---|---|---|
| strike | dip | rake | strike | dip | rake | trend | plunge | trend | plunge | |
| 61 | 70 | 144 | 166 | 57 | 25 | 116 | 8 | 19 | 39 | Papazachos & Papazachou (2003) |
| 69 | 58 | 122 | 200 | 44 | 50 | 137 | 8 | 32 | 62 | Harvard |
| 52 | 54 | 115 | 193 | 43 | 59 | 125 | 6 | 18 | 69 | USGS |
| 71 | 52 | 120 | 208 | 47 | 57 | | | | | AUTH |
| 75 | 42 | 102 | 239 | 49 | 79 | | | | | NOA – IG |
| 75 | 63 | 137 | 187 | 52 | 33 | 134 | 6 | 36 | 47 | ETH – Zurich |
| 55 | 58 | 117 | 191 | 41 | 54 | 126 | 9 | 65 | 15 | GEOSCOPE |
| 189 | 52 | 29 | 81 | 67 | 139 | 138 | 9 | 39 | 45 | MEDNET |
| 69 | 46 | 166 | 169 | 80 | 45 | | | | | KOERI |
| 48 | 60 | 105 | 200 | 33 | 65 | 127 | 14 | 353 | 71 | CPPT |
| **70** | **75** | **165** | **164** | **76** | **16** | **296** | **1** | **28** | **21** | **this study** |

and the mainshock of the studied sequence. The present determination confirms previous results (Kiratzi and Papazachos, 1995; Benetatos *et al*., 2004) suggesting that the maximum tension is directed to the inner part of the arc and is dipping almost parallel to the dip direction of the descending Mediterranean slab, while the maximum compression is almost parallel to the strike of the arc.

## 5. Shape of the Hellenic Wadati–Benioff Zone

The new approach of the present study in an effort to define more accurately the geometry of the Benioff zone in the SW part of the Hellenic arc is the relocation of the earthquakes that occurred in the area since 1964. For the division of the whole study area in subareas, following the procedure mentioned in a previous section, the 14.457 earthquakes selected from the ISC on-line bulletin were separated in clusters taking into account their focal and geographical distribution. Initially, all events were grouped into six sets according to their focal depths determined by the ISC, that is, from 0-20 km, 20-50 km, 50-70 km, 70-100 km, 100-140 km and greater than 140 km. Then, each set was further subdivided, according to the earthquakes geographical distribution, aiming to calculate different time residuals for several subareas the dimensions of which were as small as possible for the inclusion of an adequate number of events. In this way, we defined 15 sub areas and calculated the time residuals for each one in relation with the regional velocity model, following a similar procedure as for the aftershock sequence. In order to minimize the calculations resulting in lower location precision, the time residuals for only the earthquakes that occurred after 1981 were estimated, since when the regional Greek seismological network had become denser. Additional criteria concern the number of available recordings for each event (8 or more, meaning at least 7 P– and one S– arrivals) and with statistical errors of RMS≤0.9 s, ERH≤10 km and ERZ≤10 or 15 km depending on the site and the number of events comprised in the subarea. The number of the earthquakes that satisfy the above criteria is now equal to 4341. This last data sample was used for the calculation of the time residuals and the relocation of all the earthquakes comprised in the initial data sample. During this stage of the relocation the arrivals with time residuals less than 2.0 s for both the P– and S–waves were taken into account. From the relocated events the ones with more than 7 remaining P–recordings and with vertical (ERZ) and horizontal (ERH) uncertainties in the hypocenters less than 10 km, and RMS<0.8 s were considered as the best located ones, numbering 2758 in total. The epicenters of these events are depicted on the map of fig. 5a with different symbols for the shallow (circles) and the intermediate focal depth (triangles) events. Shallow seismic activity is predominant in the area, while the epicenters of the intermediate earthquakes are projected between the fore arc and the back arc area. Aiming to define the geometry of the Benioff zone, four vertical sections across the lines plotted on the map of fig. 5a were performed. In each profile the earthquakes located in an almost triangular shaped area with its base length of almost 120 km, around the lines AE, BE, CE and DE have been included with no overlapping. The orientation of the four lines, changing from almost E-W in the northwestern part of the area to almost N-S in its southeastern part, was selected to be parallel with the dip direction of the Benioff zone at each site. The four cross sections are matched and presented all together in fig. 5b. The descending slab is delineated rather clearly, sinking at an angle of about 30° up to the depth of 70 km and with a steeper angle of about 47° in larger depths. The crustal seismicity in the fore arc area is distributed in depths of 20-25 km, while along the outer part of the Hellenic trench the seismicity reaches depths of 50 km or more, although the majority of hypocenters are concentrated in shallower depths.

The asterisk and black circles on the map of fig. 6 depict the epicenters of the main shock and its aftershocks, respectively. Grey symbols represent the background seismicity as it has been plotted in fig. 5. The lower part of fig. 6 shows the cross sections as in fig. 5, including also the 2006 main shock and its aftershock

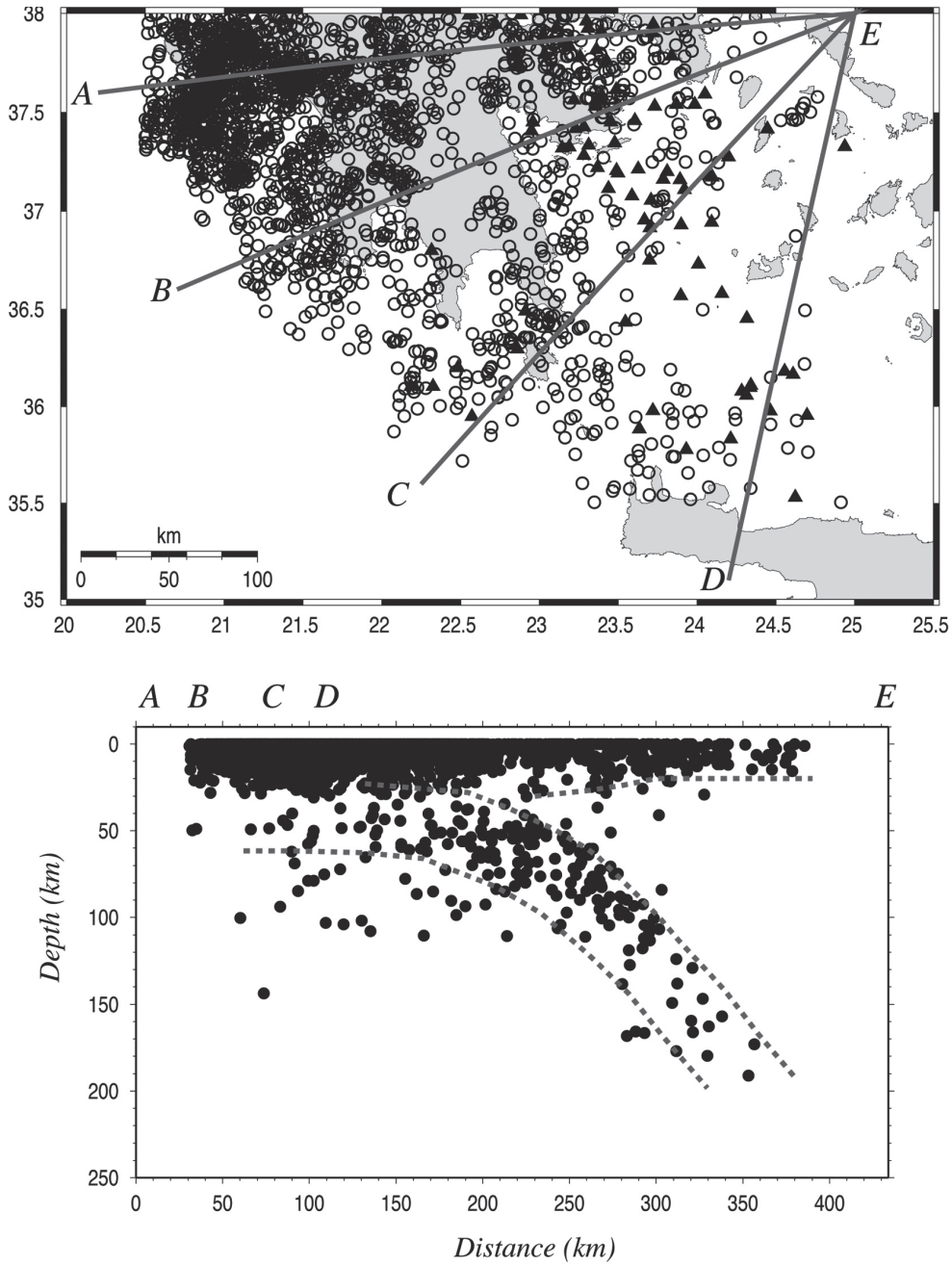


**Fig. 5a,b.** a) Map of the epicenters of all the relocated earthquakes with more than 7 P–phases and RMS≤0.8s, ERH≤10km and ERZ≤10km. Shallow seismicity is depicted by open circles, whereas and the intermediate focal depth events are represented with triangles. b) Four vertical sections across around the lines AE, BE, CE and DE are presented all together.

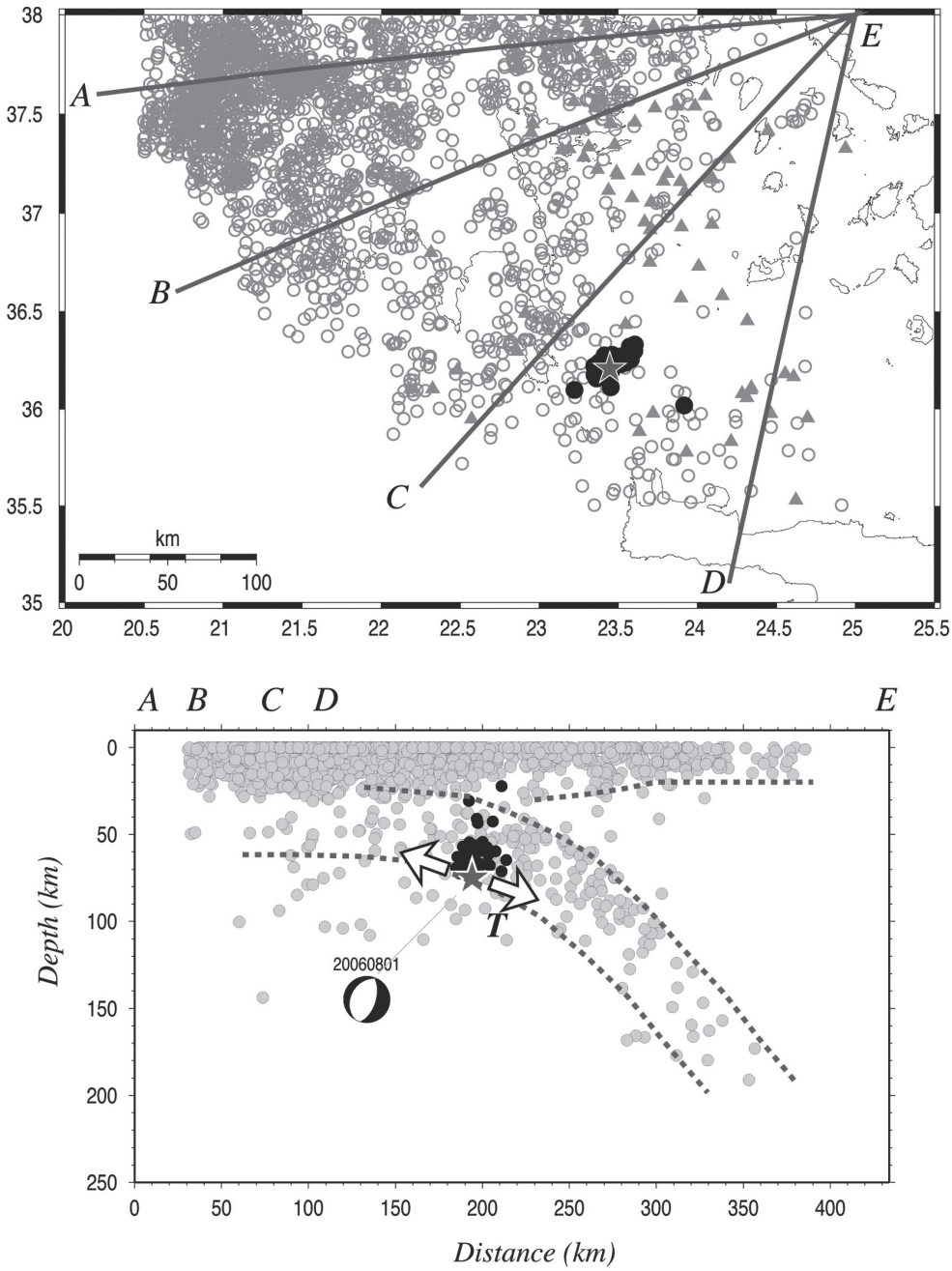


**Fig. 6.** Cross sections along the four lines, AE, BE, CE and DE including also the 2006 main shock and its aftershock sequence. Grey circles depict the background seismicity, while black circles and a star depict the foci of aftershocks and the main shock of the sequence, respectively. The focal mechanism of the main shock is shown as equal area projection of the front hemisphere.

sequence. The hypocenters of the aftershock sequence are located within the sinking slab occupying the lower part of the Benioff zone in an area where the slab becomes gradually steeper. Plot of the T–axis shows that the stress field is extensional along the slab supporting that slab-pull is the driving force for the intraplate earthquake occurrence.

## 6. Discussion and conclusions

The strong $M_w$=6.7 intermediate depth Kythira main shock along with its accurately located aftershock sequence, provided additional information on the geometry of the descending slab of the Hellenic Wadati-Benioff zone. The determination of its focal mechanism confirms along-slab tension and lateral compressional stresses at the southwestern part of the subduction zone, being in accordance with previous results. The aftershock hypocenters along with the relocated seismicity of the last decades in a broader than the aftershock area, contributed to the clarification of the subduction shape.

Hypocentral relocation was performed by Papazachos *et al*. (2000) for 961 shallow and intermediate depth earthquakes, which occurred between 1964 and 1995 in the Hellenic arc in order to define the plate boundaries in this area. They relocated the earthquakes with focal depths shallower than 100 km and used the locations of ISC for the earthquakes of larger depths. By this way, they have defined a Wadati-Benioff zone with a shallow branch (20-100 km), which is dipping at low angle (~30°) to the Aegean Sea and where an interaction of ocean–continent type occurs. Coupling between the subducted oceanic crust and the overriding of the Aegean lithospheric plate takes place on the shallow part of the subduction interface. The deep branch (100-180 km) of the Wadati-Benioff zone is dipping freely (without coupling) at a high angle (~45°) beneath the south Aegean trough and the volcanic arc. The authors claim that the location of strong deep earthquakes ($h$>100 km) in the fore–arc area of the southwestern part of the Hellenic arc (west of Kythira) indicates that oceanic crust is «destroyed» in this part of the Hellenic trench due to roll-back of the descending lithospheric slab.

Although the present study is in agreement with Papazachos *et al*. (2000), it provides more robust results for the geometry and the properties of the Wadati-Benioff zone, since much more data, 2758 events in the present paper, are used for this scope and the relocation is extended to all depth ranges. The present relocation, which reveals the continuation of the hypocentral distribution along the entire slab, provides also the definition of the thickness of the subducting slab which was found equal to about 45 km.

At the interface of the subducting and the overriding plates thrust-faulting earthquakes are located, while intraplate events occur inside the downgoing slab. The main event examined in the current study is an intraslab strike slip earthquake that occurred at ~75 km depth, located below the downdip edge of the seismogenic coupled interface, on a subvertical plane, revealing lateral slab tearing. In the present case, coupling is considerably weak (~0.10) and the coupling interface is at a depth of about 50 km (Papadimitriou and Karakostas, 2005). Intermediate depth events in the area are of strike slip faulting (Papazachos *et al*., 2000), slab pull events (down-dip tensional) and compressional parallel to the strike of the subduction front), expressing slab bending, which as it sinks it forms an amphitheatrical shape. The main shock faulting type is in accordance with relevant observations in global scale. Lay *et al*. (1989) found that with the exception of Tonga, the intermediate depth activity in most regions of the world is dominated by down-dip tensional mechanisms, which reflect the negative buoyancy and tensile coherence of the lithosphere. Down-dip tensional stresses within the subduction plate have also found for the most large (M>6.8) intermediate-depth earthquakes occurring down-dip of strongly coupled subduction zones (Astiz *et al*., 1984).

## Acknowledgements

The GMT system (Wessel and Smith, 1998) was used to plot the figures. Usage of data from

GFZ Potsdam is also acknowledged. This work was supported by the «Pythagoras» project funded by the EPEAEK. Geophysics Department contribution 735.

*REFERENCES*


ALESSANDRINI, B., L. BERANZOLI, G. DRAKATOS, C. FALCONE, G. KARANTONIS, F.M. MELE and G. STAVRAKAKIS (1997): Back arcs basins and P–wave crustal velocity in the Ionian and Aegean regions, *Geophys. Res. Lett.*, **24**, 527-530.

ASTIZ, L., T. LAY and H. KANAMORI (1984): A global study of intermediate depth earthquake mechanisms. EOS, *Trans. Am. Geophys. Union*, **65**, 1015.

BENETATOS, C., A. KIRATZI, C. PAPAZACHOS and G. KARAKAISIS (2004): Focal mechanisms of shallow and intermediate depth earthquakes along the Hellenic Arc, *J. Geodyn.*, **37**, 253-296.

BOHNHOFF, M., H.-P. HARJES and T. MEIER (2005): Deformation and stress regimes in the Hellenic subduction zone from focal Mechanisms, *J. Seismology*, **9**, 341-366.

DE CHABALIER, J., H. LYON–CAEN, A. ZOLLO, A. DESCHAMPS, P. BERNARD and D. HATZFELD (1992): A detailed analysis of microearthquakes in western Crete from digital three-component seismograms, *Geophys. J. Int.*, **110**, 347-360.

GEOFON, http://www.gfz-potsdam.de/geofon/www_req/gfn_data.html.

HATZFELD, D., G. PEDOTTI, P. HATZIDIMITRIOU, D. PANAGIOTOPOULOS, M. SCORDILIS, I. DRAKOPOULOS, K. MAKROPOULOS, N. DELIBASIS, I. LATOUSAKIS, J. BASKOUTAS and J. FROGNEUX (1989): The Hellenic subduction beneath the Peloponnesus: first results of a microearthquake study, *Earth Plan. Sc. Lett.*, **93**, 283-291.

HATZFELD, D., G. PEDOTTI, P. HATZIDIMITRIOU and K. MAKROPOULOS (1990): The strain pattern in the western Hellenic arc deduced from a microearthquake survey, *Geophys. J. Int.*, **101**, 181-202.

HATZFELD, D. and C. MARTIN (1992): Intermediate depth seismicity in the Aegean defined by teleseismic data, *Earth Plan. Sc. Lett.*, **113**, 267-275.

INTERNATIONAL SEISMOLOGICAL CENTRE (2001): *On-line Bulletin*, http://www.isc.ac.uk/ Bull, Internat. Seis. Cent., Thatcham, United Kingdom.

ITSAK (2006): The Kythira (Greece) earthquake of January 8, 2006: Preliminary report on strong motion data, Geotechnical and Structural damage, Hell. Min. of Environment, Phys. Planning, and Public Works.

KAHLE, H., D. STRAUB, R. REILINGER, S. MCCLUSKY, R. KING, K. HURST, G. VEIS, K. KASTENS and P. CROSS (1998): The strain rate field in the eastern Mediterranean region, estimated by repeated GPS measurements, *Tectonophysics*, **294**, 237-252.

KIRATZI, A. and C.B. PAPAZACHOS (1995): Active deformation of the shallow part of the subducting lithospheric slab in the southern Aegean, *J. Geodyn.*, **19**, 65-78.

KLEIN, F. (2002): User's Guide to HYPOINVERSE–2000, a Fortan program to solve for earthquakes locations and magnitudes, Open file report 02-171, USGS.

KNAPMEYER, M. (1999): Geometry of the Aegean Benioff zone, *Ann. Geofisica*, **42**, 27-38.

LAY, T., L. ASTIZ, H. KANAMORI and D. CHRISTENSEN (19899: Temporal variation of large intraplate earthquakes in coupled subduction zones, *Phys. Earth Plan. Int.*, **54**, 258-312.

LE PICHON, X. and J. ANGELIER (1979): The Aegean arc and trench system: a key to the neotectonic evolution of the eastern Mediterranean area, *Tectonophysics*, **60**, 1-42.

NIKOLINTAGA, I., V. KARAKOSTAS, E. PAPADIMITRIOU and F. VALLIANATOS (2007): Velocity models inferred from P-waves travel time curves in South Aegean, *Bull. Geol. Soc. Greece*, XXXX, 1187-1198.

PANAGIOTOPOULOS, D. and B. PAPAZACHOS (1985): Travel times of Pn waves in the Aegean and surrounding area, *Geophys. J. R. Astron. Soc.*, **80**, 165-176.

PAPADIMITRIOU, E. and V. KARAKOSTAS (2005): Faulting geometry and seismic coupling of the southwest part of the Hellenic subduction zone, Abstract in 33rd IASPEI Gen. Ass., Santiago, Chile, 2-8 October 2005.

PAPAZACHOS, B.C. (1990): Seismicity of the Aegean and surrounding area, *Tectonophysics*, **178**, 287-308.

PAPAZACHOS, B.C. and P.E. COMNINAKIS (1970): Geophysical features of the Greek island arc and eastern Mediterranean ridge, Com. Ren. des Séances de la Conférence Réunie à Madrid, 1969, **16**, 74-75.

PAPAZACHOS, B.C. and P.E. COMNINAKIS (1971): Geophysical and Tectonic Features of the Aegean arc., *J. Geophys. Res.*, **76**, 8517-8533.

PAPAZACHOS, B.C. and C.B. PAPAZACHOU (2003): *The Earthquakes of Greece*, (Ziti publ., Thessaloniki, Greece), pp. 317.

PAPAZACHOS, B.C., E.E. PAPADIMITRIOU, A.A. KIRATZI, C.B. PAPAZACHOS and E.K. LOUVARI (1998): Fault plane solutions in the Aegean and the surrounding area and their tectonic implications, *Boll. Geof. Teor. Appl.*, **39**, 199-218.

PAPAZACHOS, B., V. KARAKOSTAS, C. PAPAZACHOS and E. SCORDILIS (2000): The geometry of the Wadati-Benioff zone and lithospheric kinematics in the Hellenic arc, *Tectonophysics*, **319**, 275-300.

PAPAZACHOS, B., E. SCORDILIS, D. PANAGIOTOPOULOS, C. PAPAZACHOS and G. KARAKAISIS (2004): Global Relations between seismic fault parameters and moment magnitude of Earthquakes, *Bull. Geol. Soc. Greece*, **XXXVI**, 1482-1489.

PAPAZACHOS, C., P. HATZIDIMITRIOU, D. PANAGIOTOPOULOS and G. TSOKAS (1995): Tomography of the crust and upper mantle in Southeast Europe, *J. Geophys. Res.*, **100**, 405-422.

PAPAZACHOS, C.B. and G. NOLET (19979: P and S deep velocity structure of the Hellenic area obtained by robust nonlinear inversion of travel times, *J. Geophys. Res.*, **102**, 8349-8367.

PAPAZACHOS, C.B., G.F. KARAKAISIS, A.S. SAVVAIDIS and B.C. PAPAZACHOS (2002): Accelerating Seismic Crustal Deformation in Southern Aegean Area, *Bull. Seismol. Soc. Am.*, **92**, 570-580.

REASENBERG, P.A. and D. OPPENHEIMER (1985): FPFIT, FPPLOT, and FPPAGE: Fortran computer programs for calculating and displaying earthquake fault-plane solutions, U.S. Geol. Surv. Open-File Rep. 85-739.

SONDER, L. and P. ENGLAND (1986): Vertical averages of rheology of the continental lithosphere: relation to thin sheet parameters, *Earth Plan. Sc. Lett.*, **77**, 81-90.

TZANIS, A. and F. VALLIANATOS (2003): Distributed power–law seismicity changes and crustal deformation in the SW Hellenic arc, *Nat. Haz. Earth Syst. Sc.*, **3**, 179-198.

WELLS, D. and K. COPPERSMITH (1994): New empirical relationships among magnitude, rupture length, rupture width, rupture area, and surface displacement, *Bull. Seism. Soc. Am.*, **84**, 974-1002.

WESSEL, P. and W.H.F. SMITH (1998): New, improved version of the Generic Mapping Tools Released. EOS Trans. AGU 79, pp. 579.

WORTEL, M. and W. SPAKMAN (2000): Subduction and Slab Detachment in the Mediterranean – Carpathian Region. Science, **290**, 1910-1917.

(received March 1, 2008;
accepted June 15, 2008)